Magnetohydrodynamic flow with heat and mass transfer of non-Newtonian fluid past a vertical heated plate embedded in non-Darcy porous medium with variable porosity

N. T. Eldabe,

Department of Mathematics, Faculty of Education, Ain Shams University,Cairo, Egypt

M. Abu Zeid*,

Basic Science Department, Higher Technological Institute, 10 th of Ramadan City, Egypt * E-mail of the corresponding author: abuzeid71@yahoo.com

Abstract

Numerical solutions of the nonlinear partial differential equations which describe the motion of the non-Newtonian fluid with heat and mass transfer past a semi-infinite vertical heated plate embedded in a porous medium are obtained. The considered fluid is obeying the Eyring Powell model. The system is stressed by an external uniform magnetic field. The porous medium is obeying the non-Darcy Forchheimer model. The variation of permeability, porosity and thermal conductivity are considered. Similarity transformations are made to transform the system of equations to non-linear ordinary differential equations. A shooting algorithm with Runge-Kutta Fehlberg integration scheme is used to solve these equations. The velocity, temperature and concentration distributions are obtained as functions of the physical parameters of the problem. The effects of these parameters on these distributions are discussed and illustrated graphically through a set of figures.

Keywords: Magnetohydrodynamics, Mixed convection, Eyring Powell model, Non- Darcy flow, Porous medium, Magnetic field.

1. Introduction

Non-Newtonian fluids are of great commercial importance. Such fluids include slurries, shampoo, cosmetic products, toothpaste, clay coating and suspensions, grease, and many others. Magnetohydrodynamics (MHD) plays an important role in agriculture, engineering and petroleum industries. The problem of mixed convection under the influence of magnetic field has attracted numerous researchers in view of its applications in astrophysics, and in the geophysics. Chen [1] analyzed the combined heat and mass transfer of an electrically conducting fluid in MHD natural convection adjacent to a vertical surface. Pravin et al. [2] studied boundary layer flow behaviour with non-darcy forced and MHD free convection and mass transfer flow of an incompressible viscous fluid past a continuously moving infinite vertical porous plate in the presence of large suction and under the influence of uniform magnetic field considering heat source and thermal diffusion. Alam and Sattar [3] analyzed the transient MHD heat and mass transfer flow in a rotating system in presence of thermal diffusion. Hung and Chen [4] have studied non-Darcy free convection in a thermally stratified fluid saturated porous medium along a vertical plate with variable heat flux. Ferdows et al. [5] studied the effect of the large suction on the MHD forced and free convection flow past a vertical porous plate.

Mohammadein and El-Shaer [6] studied mixed convective flow past a semi-infinite vertical plate embedded in a porous medium incorporating the variable permeability in Darcy's model. Elbashbeshy and Bazid [7] studied heat transfer in a porous medium over a stretching surface with internal heat generation and suction or injection. Zhang et al. [8] presented transientand steady natural convection from a heat source embedded in a saturated porous layer. Alam et al. [9] studied the effects of Dufour and Soret numbers on steady combined free-forced convective and mass transfer flow past a semi-infinite vertical flat plate Makind in the presence of an uniform transverse magnetic field. Makinde [10] examined the MHD boundary layer flow and mass transfer past a vertical plate in a porous medium with constant heat flux. Pal [11] studied the effects of Forchheimer inertial terms, buoyancy parameter, thermal conductivity ratio, variable porosity, viscous dissipation on mixed convection heat transfer past a semi-infinite vertical plate embedded in a saturated porous medium in the presence of magnetic field. Elbashbeshy and Bazid [12] studied the mixed convection along a vertical plate with variable surface embedded in porous medium. Kumar [13] studied radiation and viscous dissipation effects over a stretching surface subjected to variable heat flux in presence of transverse magnetic field.

The study of electrically conducting non-Newtonian fluids flowing under the influence of external magnetic field has become of principal interest because magnetic forces produced in it influence the motion of the fluids in significant manner and such interaction problems have great practical applications. Eldabe and Sallam [14] studied the flow and heat transfer in the non-Newtonian visco-elastic electrically conducting incompressible porous fluid medium confined between two parallel plates; one of them is a stretching plate and

the other is a stationary porous plate through which there is a uniform injection. Veena et al. [15] investigated the study of non-similar solutions for an electrically conducting visco-elastic fluid flow with heat and mass transfer over a stretching sheet embedded in saturated porous medium.

Motivated by all these studies we investigate Magnetohydrodynamic flow with heat and mass transfer of non-Newtonian fluid past a vertical heated plate embedded in non-Darcy porous medium with variable porosity. The nonlinearity of the basic equations and additional mathematical difficulties associated with solving it, have led us to use numerical method. The transformed dimensionless governing equations are solved numerically by using fifth-order Runge-Kutta-Fehlberg method (RKF45) with shooting technique. The effects of various physical parameters on velocity, heat and mass transfer are analyzed.

2. Mathematical formulation of the problem

We consider two-dimensional steady flow of a laminar incompressible non-Newtonian and electrically conducting fluid past a semi-infinite vertical heated plate embedded in a saturated porous medium of variable porosity, permeability and thermal conductivity. Introducing Cartesian co-ordinate system, x-axis is chosen along the plate and y-axis normal to it (see figure 1). A uniform transverse magnetic field of strength $\vec{B} = (0, B_0, 0)$ is applied to the plate. In accordance with the boundary layer theory, Lorentz and pressure forces with inertia play an important role.

The analysis is based on the following assumptions:

i) The magnetic Reynolds number is assumed to be small, so that the induced magnetic field is negligible.
ii) The plate is assumed to be electrically non-conducting.
iii) The convecting fluid and the porous medium are everywhere in thermo-dynamic equilibrium.
iv) Darcy resistance and quadratic drag terms are taken into account.
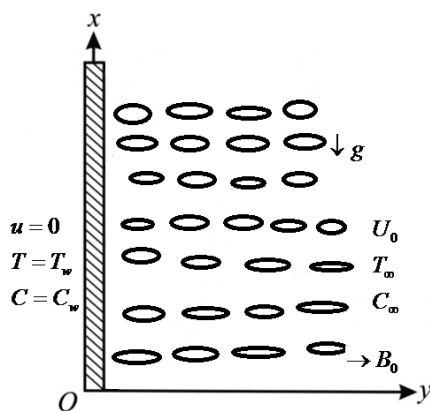v) The viscous dissipation term has been taken into account.

Figure (1). Physical model of the problem.

With the above assumptions the governing equations relevant to the problem are:
The equation of continuity

$$\frac{\partial u}{\partial x} + \frac{\partial v}{\partial y} = 0 \qquad (1)$$

The equation of momentum

$$u \frac{\partial u}{\partial x} + v \frac{\partial u}{\partial y} = -\frac{1}{\rho} \frac{\partial P}{\partial x} + g\beta(T - T_\infty) + g\beta^*(C - C_\infty) + \frac{1}{\rho} \frac{\partial}{\partial y}(\tau_{xy}) - \frac{\mu \varepsilon(y)}{\rho k(y)} u$$
$$- \frac{C_b \varepsilon^2(y)}{\sqrt{k(y)}} u^2 - \frac{\sigma_m B_0^2}{\rho} u \qquad (2)$$

The equation of energy

$$u\frac{\partial T}{\partial x} + v\frac{\partial T}{\partial y} = \frac{\partial}{\partial y}\left(\alpha(y)\frac{\partial T}{\partial y}\right) + u\left[\frac{\mu\varepsilon(y)}{\rho c_p k(y)}u + \frac{C_b\varepsilon^2(y)}{\sqrt{k(y)}c_p}u^2 - \frac{\mu}{\rho c_p}\frac{\partial^2 u}{\partial y^2}\right] + \frac{\sigma_m B_0^2}{\rho c_p}u^2 \qquad (3)$$

The equation of mass diffusion

$$u\frac{\partial C}{\partial x} + v\frac{\partial C}{\partial y} = D\frac{\partial^2 C}{\partial y^2} \qquad (4)$$

Where u and v are the velocity components along the x- and y- directions, respectively, P is the fluid pressure, g is the gravitational field downward, τ_{xy} is the stress tensor in the classical nonpolar theory, ρ is the fluid density, μ is the fluid viscosity, $k(y)$ is the variable permeability of the porous medium, $\varepsilon(y)$ is the porosity of the saturated porous medium, $\alpha(y)$ is the variable effective thermal diffusivity of the medium, C_b is the empirical constant of the second-order resistance term due to inertia effect, c_p is the specific heat at constant pressure, β is the thermal expansion coefficient, β^* is the concentration expansion coefficient, B_0 is the applied magnetic field, σ_m is the electrical conductivity, T is the temperature of the fluid, T_∞ is the free stream temperature, C is the concentration of the fluid, C_∞ is the free stream concentration, D is the molecular diffusivity. For a non-Newtonian fluid obeying the Eyring Powell model we have

$$\tau_{xy} = \mu\frac{\partial u}{\partial y} + \frac{1}{A^*}\sinh^{-1}(\frac{1}{c}\frac{\partial u}{\partial y}) \qquad (5)$$

Where A^* and c are the characteristics of the Eyring-Powell model.

We take the first and second order approximation of the $\sinh^{-1}(\frac{1}{c}\frac{\partial u}{\partial y})$ function:

$$\sinh^{-1}(\frac{1}{c}\frac{\partial u}{\partial y}) \cong \frac{1}{c}\frac{\partial u}{\partial y} - \frac{1}{6}(\frac{1}{c}\frac{\partial u}{\partial y})^3 \quad , \quad \left|\frac{1}{c}\frac{\partial u}{\partial y}\right| < 1 \qquad (6)$$

Then equation (2) becomes

$$u\frac{\partial u}{\partial x} + v\frac{\partial u}{\partial y} = -\frac{1}{\rho}\frac{\partial P}{\partial x} + g\beta(T - T_\infty) + g\beta^*(C - C_\infty) + \frac{\mu}{\rho}\frac{\partial^2 u}{\partial y^2} + \frac{1}{\rho A^* c}\frac{\partial^2 u}{\partial y^2}$$

$$-\frac{1}{2\rho A^{*} c^3}\left(\frac{\partial u}{\partial y}\right)^2\frac{\partial^2 u}{\partial y^2} - \frac{\mu\varepsilon(y)}{\rho k(y)}u - \frac{C_b\varepsilon^2(y)}{\sqrt{k(y)}}u^2 - \frac{\sigma_m B_0^2}{\rho}u \qquad (7)$$

The appropriate boundary conditions are

$$u = 0, \quad v = 0, \quad T = T_w, \quad C = C_w \quad \text{at} \quad y = 0 \qquad (8)$$

$$u = U_0, \quad v = 0, \quad T = T_\infty, \quad C = C_\infty \quad \text{as} \quad y \to \infty \qquad (9)$$

At a sufficiently large distance from the porous surface the flow field is uniform, so in the free stream, $u = U_0$, $T = T_\infty$, $C = C_\infty$, where U_0 is the free stream velocity, then equation (7) reduces to

$$\frac{1}{\rho}\frac{\partial P}{\partial x} = -\frac{\mu\varepsilon(y)}{\rho k(y)}U_0 - \frac{C_b\varepsilon^2(y)}{\sqrt{k(y)}}U_0^2 - \frac{\sigma_m B_0^2}{\rho}U_0 \tag{10}$$

Using eq. (10) for eliminating $\dfrac{\partial P}{\partial x}$ in eq. (7), we get the momentum equation as follows:

$$u\frac{\partial u}{\partial x} + v\frac{\partial u}{\partial y} = g\beta(T - T_\infty) + g\beta^*(C - C_\infty) + \frac{\mu}{\rho}\frac{\partial^2 u}{\partial y^2} + \frac{1}{\rho A^* c}\frac{\partial^2 u}{\partial y^2} - \frac{1}{2\rho A^* c^3}\left(\frac{\partial u}{\partial y}\right)^2\frac{\partial^2 u}{\partial y^2}$$
$$+ \frac{\mu\varepsilon(y)}{\rho k(y)}(U_0 - u) + \frac{C_b\varepsilon^2(y)}{\sqrt{k(y)}}(U_0^2 - u^2) + \frac{\sigma_m B_0^2}{\rho}(U_0 - u) \tag{11}$$

And eq. (3) becomes

$$u\frac{\partial T}{\partial x} + v\frac{\partial T}{\partial y} = \frac{\partial}{\partial y}\left(\alpha(y)\frac{\partial T}{\partial y}\right) + u\left[\left(\frac{\mu\varepsilon(y)}{\rho c_p k(y)} + \frac{\sigma_m B_0^2}{\rho c_p}\right)(u - U_0)\right.$$
$$\left. + \frac{C_b\varepsilon^2(y)}{\sqrt{k(y)}c_p}(u^2 - U_0^2) - \frac{\mu}{\rho c_p}\frac{\partial^2 u}{\partial y^2}\right] \tag{12}$$

To solve the above system of equations (11), (12), and (4) under the boundary conditions (8-9) we adopt the well-defined similarity technique to obtain the similarity solutions.

For this purpose the following similarity variables are introduced:

$$\eta = \left(\frac{y}{x}\right)\left(\frac{U_0 x}{\upsilon}\right)^{\frac{1}{2}}, \quad \psi = \sqrt{\upsilon U_0 x}\, f(\eta), \quad \theta(\eta) = \frac{T - T_\infty}{T_w - T_\infty}, \quad \phi(\eta) = \frac{C - C_\infty}{C_w - C_\infty} \tag{13}$$

Where $\psi(x, y)$ is the stream function, η is the similarity variable, f is the dimensionless stream function, and θ and ϕ are the dimensionless temperature and concentration variables, respectively. T_w is the plate temperature with, $T_w > T_\infty$ and C_w is the concentration at the plate surface with $C_w > C_\infty$.

The continuity equation is satisfied by $u = \dfrac{\partial \psi}{\partial y}$ and $v = -\dfrac{\partial \psi}{\partial x}$, and the velocity components are:

$$u = U_0 f'(\eta) \quad \text{and} \quad v = -\frac{1}{2}\sqrt{\frac{\upsilon U_0}{x}}\left[f(\eta) - \eta f'(\eta)\right] \tag{14}$$

Where a prime represents differentiation with respect to η.

We consider the variable permeability $k(\eta)$, variable porosity $\varepsilon(\eta)$ and the variable thermal diffusivity $\alpha(\eta)$ [11] as follows:

$$k(\eta) = k_0(1 + d\, e^{-\eta}) \tag{15}$$

$$\varepsilon(\eta) = \varepsilon_0(1 + d^* e^{-\eta}) \tag{16}$$

$$\alpha(\eta) = \alpha_0\left[\varepsilon_0(1 + d^* e^{-\eta}) + \sigma^*\left\{1 - \varepsilon_0(1 + d^* e^{-\eta})\right\}\right] \tag{17}$$

Where k_0, ε_0 and α_0 are the permeability, porosity and thermal diffusivity at the edge of the boundary layer, respectively and σ^* is the ratio of the thermal conductivity of solid to the conductivity of the fluid. For variable porosity and permeability (VP) where d and d^* are treated as constants having values 3.0 and 1.5, respectively, and for uniform porosity and permeability (UP) where, $d = d^* = 0$.

Substituting eqs. (13) and (14) into eqs. (11), (12) and (4) and using (15-17), we obtain:

$$(1+M^*)f''' - D^*\operatorname{Re}^2 f''^2 f''' + \frac{1}{2}f f'' + \frac{Gr}{\operatorname{Re}^2}\theta + \frac{Gm}{\operatorname{Re}^2}\phi + \left(\frac{1}{\sigma\operatorname{Re}}\right)\frac{1+d^*e^{-\eta}}{1+de^{-\eta}}(1-f')$$

$$+ M^2(1-f') + \frac{\beta'(1+d^*e^{-\eta})^2}{(1+de^{-\eta})^{1/2}}(1-f'^2) = 0 \qquad (18)$$

$$\left[\varepsilon_0 + \sigma^*(1-\varepsilon_0) + \varepsilon_0 d^*e^{-\eta}(1-\sigma^*)\right]\theta'' + \frac{1}{2}\operatorname{Pr} f\theta' + \varepsilon_0 d^*e^{-\eta}(\sigma^*-1)\theta'$$

$$+ \operatorname{Pr}Ec\left[\left(\frac{1}{\sigma\operatorname{Re}}\frac{1+d^*e^{-\eta}}{1+de^{-\eta}}+M^2\right)(f'-1) + \frac{\beta'(1+d^*e^{-\eta})^2}{(1+de^{-\eta})^{1/2}}(f'^2-1) - f'''\right] = 0 \qquad (19)$$

$$\phi'' + \frac{1}{2}Sc f \phi' = 0 \qquad (20)$$

Where $M^* = 1/\mu A^* c$ and $D^* = U_0/2\rho A^* c^3 x^3$ represent the non-Newtonian effects, which vanish in Newtonian flows, $\beta' = C_b \varepsilon_0^2 x/k_0^{1/2}$ is the local inertial parameter, $\operatorname{Pr} = \mu/(\rho\alpha_0)$ is the Prandtl number, $Ec = U_0^2/\{c_p(T_w - T_\infty)\}$ is the Eckert number, $\sigma = k_0/(x^2\varepsilon_0)$ is the local permeability parameter, $\operatorname{Re} = U_0 x/\upsilon$ is the local Reynolds number, $Gr = g\beta(T_w - T_\infty)x^3/\upsilon^2$ is the local temperature Grashof number, $Gm = g\beta^*(C_w - C_\infty)x^3/\upsilon^2$ is the local concentration Grashof number, $M^2 = \sigma_m B_0^2 x/(\rho U_0)$ is the local magnetic field parameter and $Sc = \upsilon/D$ is the Schmidt number. The transformed boundary conditions are:

$$f = 0, \quad f' = 0, \quad \theta = 1, \quad \phi = 1 \quad \text{at } \eta = 0 \qquad (21)$$

$$f' = 1, \quad \theta = 0, \quad \phi = 0 \qquad \text{as } \eta \to \infty \qquad (22)$$

The flow equation (18) which is coupled with the energy and concentration equations (19) and (20) are solved using fifth-order Runge-Kutta-Fehlberg method (RKF45) with shooting technique. The most important factor of this method is to choose the appropriate finite values of $\eta \to \infty$ for the boundary value problem stated by eqs. (18), (19), and (20). To select η_∞, we begin with some initial guess value and solve the problem with some set of physical parameters to obtain $f''(0)$ and $\theta'(0)$. The solution procedure is repeated with another large (or small) value of η_∞ until two successive values for both $f''(0)$ and $\theta'(0)$ differ only by the specified significant digit. The last value of η_∞ is chosen as appropriate value for that particular set of parameters. Convergence is achieved only when the absolute vale of every one of f', θ, ϕ for last two approximations differ only by 10^{-6} at all values of η in $0 < \eta_\infty < \infty$. The numerical solutions thus obtained are displayed in tables and figures in the following section.

3. Results and discussion

The problem of two-dimensional steady flow of a laminar viscous incompressible non-Newtonian and electrically conducting fluid past a semi-infinite vertical heated plate embedded in a fluid saturated porous medium of variable porosity, permeability and thermal conductivity has been formulated, analyzed and solved numerically using fifth-order Runge-Kutta-Fehlberg method with shooting technique.

The effects of the flow parameters on the velocity, temperature and concentration distributions of the flow field are presented with the help of velocity profiles, (Figures (2)-(6)), temperature profiles (Figures (7)-(12)) and concentration profiles (Figures (13)-(18)). Figure 2 illustrates the influence of first order approximation parameter M^* on the velocity distribution. It is observed that the velocity decreases with

increasing M^* for both UP and VP cases. The boundary layer thickness increases with increasing M^*. The velocity profiles for UP are less compared to VP. Figure 3 represents the graph of velocity profile for different values of magnetic parameter M for VP. It is seen that, increases in the value of magnetic parameter M is to increase velocity profile within the boundary layer also, the boundary layer thickness increases with decreases in the value of M. This is due to the fact that the magnetic field produces Lorentz force which reduces frictional resistance and so the values of velocity profiles increased. Figure 4 displays the variation of velocity profile for various values of inertial parameter $\beta^{/}$ for VP. It is observed that, decreases in the value of $\beta^{/}$ produces a decrease in the velocity profile within the boundary layer due the resistance to the fluid flow by the porous medium. It is noted that boundary layer thickness decreases with an increase in the value of inertial parameter. Figure 5 shows the variations of velocity distribution for different values of the parameter Gr/Re^2 for both cases of UP and VP. It is observed from the figure that an increase in the value of Gr/Re^2 is to increase the velocity distribution for both UP and VP cases. This is because of temperature gradients which lead to the increase of velocity profiles. It is also seen that the velocity distribution affected by VP when Gr/Re^2 is increased. The boundary layer decreases with increases in the value of Gr/Re^2. The velocity profiles become peaked near the wall when Gr/Re^2 is increased. Figure 6 shows the variations of velocity distribution for different values of the parameter Gm/Re^2 for both cases of UP and VP. It is seen from the figure that an increase in the value of Gm/Re^2 is to increase the velocity distribution for both UP and VP cases. This is due to the fact that buoyancy force enhances fluid velocity. The velocity is less for UP than VP for certain values of Gm/Re^2. The boundary layer thickness decreases with increases in the value of Gm/Re^2.

Figure 7 illustrates the effect of first order approximation parameter M^* on the temperature profiles. It is noticed from the figure that the temperature profiles increase with increasing values of M^* in the boundary layer for both UP and VP cases. The effect of increasing M^* is to increase the boundary layer thickness and the temperature for VP is less compared to UP case. Figure 8 represents the temperature profiles for different values of magnetic parameter M for VP. It is noticed that the temperature profile decreases with an increase in M and the thickness of the thermal boundary layer reduces. Figure 9 displays temperature profile for various values of second-order resistance $\beta^{/}$ for variable permeability VP. It is seen that the effect of increasing $\beta^{/}$ is to decrease temperature throughout the boundary layer which results in decrease in the thermal boundary layer thickness.

Figure 10 represents the graph of temperature profile for different values of Gr/Re^2 for both the cases of UP and VP. This figure shows that an increase in the buoyancy parameter Gr/Re^2 leads to a decrease in the temperature profile. The temperature profiles for VP are less compared to UP. The thickness of the boundary layer decreases with increasing the buoyancy parameter Gr/Re^2. Figure 11 represents temperature profile for different values of Gm/Re^2 for both the cases of UP and VP. The figure shows that an increase in the parameter Gm/Re^2 is to decrease the temperature profile and thickness of the boundary layer decreases. The temperature profiles for VP are less compared to UP. Figure 12 represents the graph of temperature profile for various values of Prandtl number *Pr* for both UP and VP cases. It is seen that the effect of increasing Pr is to decrease temperature throughout the boundary layer which results in decrease in the thermal boundary layer thickness for both UP and VP cases and temperature for VP is always less compared to UP case. The rate of cooling is much faster for higher values of *Pr*. The effect of first order approximation parameter M^* on the concentration profiles is shown in fig. 13. It is noticed that concentration increases with increase in M^* for both UP and VP cases. The boundary layer thickness increases with increasing the value of M^*.

The effect of Schmidt number Sc on concentration distribution for VP is shown in fig. 14. It is noticed from the graph that increasing the value of Schmidt number decreases the concentration of species in the boundary layer. An increase in the Schmidt number produces decrease in the concentration boundary layer thickness. Physically, the increase in the value of Sc means decrease of molecular diffusion *D*. Figure 15, Shows that the concentration decreases with increasing the magnetic parameter M, and the concentration boundary layer thickness decreases. In fig. 16, the concentration decreases with increasing second-order

resistance $\beta^{/}$ and concentration boundary layer thickness decreases. Figures 17 and 18 Show that concentration decreases with increasing parameters, Gr / Re^2 and Gm / Re^2, respectively.

4. Conclusions

In this study, a numerical analysis is carried out to discuss the motion of non-Newtonian fluid with heat and mass transfer through a non-Darcian porous medium past a vertical plate. The conservation equations that govern the problem are reduced to a system of non-linear ordinary differential equations by using similarity transformations. These equations are more conveniently solved numerically by Runge-Kutta-Fehlberg method with shooting technique. We found some of the important results from the graphical representation which are listed below.

(1) Increasing the first order approximation parameter M^{*} leads to a decrease in velocity distribution, while reverse effect is observed by increasing the thickness in the boundary layer.

(2) Velocity increases with increase in the magnetic parameter M, the inertial parameter $\beta^{/}$ for VP and the buoyancy parameter Gr / Re^2, the parameter Gm / Re^2, for both UP and VP and decreases the boundary layer thickness.

(3) Increasing the first order approximation parameter M^{*} leads to an increase in temperature distribution.

(4) Temperature decreases with increase in the magnetic parameter M, the inertial parameter $\beta^{/}$, the buoyancy parameter Gr / Re^2, the parameter Gm / Re^2 and the Prandtl number Pr and decrease the thermal boundary layer thickness.

(5) Concentration distribution for both UP and VP cases decreases with decrease in the first order approximation parameter M^{*}. The boundary layer thickness increases with increasing M^{*}.

(6) Concentration decreases with increase in the Schmidt number Sc, the magnetic parameter M, the inertial parameter $\beta^{/}$, the buoyancy parameter Gr / Re^2, and the parameter Gm / Re^2, for VP case and the boundary layer thickness decreases.

References

[1] Chen, C. H., Combined Heat and Mass Transfer in MHD Free Convection from a Vertical Surface with Ohmic Heating and Viscous Dissipation, *Int. J. of Eng. Sci., 42* (2004),7, pp. 699-713

[2] Pravin, V. K., *et al*., Non-Darcy Forced Convection and MHD Free Convective Mass Transfer Flow with Heat Source and Thermal Diffusion Over a Stretching Sheet Embedded in a porous Medium, *International J. of Dynamics of Fluids, 4* (2008), 1, pp.29-42

[3] Alam, M. M., Sattar, M. A., Transient MHD heat and mass transfer flow with thermal diffusion in a rotating system, *J. Energy, Heat and Mass Transfer, 21* (1999), pp. 9-21

[4] Hung, C. I., Chen, C. B., Non-Darcy free convection in a thermally stratified porous medium along a vertical plate with variable heat flux, *Heat Mass Transfer 33* (1997), 101-107

[5] Ferdows, M., *et al.,* Similarity solutions for MHD flow through vertical porous plate with suction, *J. Comp. Appl. Mech., 6* (2005), 1, pp. 15-25

[6] Mohammadein, A. A., El-Shaer, N. A., Influence of variable permeability on combined free and forced convection flow past a semi-infinite vertical plate in a saturated porous medium, *Heat Mass Transfer 40* (2004), pp. 341-346

[7] Elbashbeshy, E. M. A., Bazid, M. A. A., Heat Transfer in a Porous Medium over a Stretching Surface with Internal Heat Generation and Suction or Injection, *Appl. Math. Comp., 158* (2004), pp. 799-807

[8] Zhang, J., *et al*., Transient and steady natural convection from a heat source embedded in thermally stratified porous layer, *Int. J. Thermal Sci., 49* (2010), 9, pp. 1527-1535

[9] Alam, M., *et al*., Dufour and Soret effects on steady MHD combined free-forced convective and mass transfer flow past a semi-infinite vertical plate, *Thammasat Int. J. Sci. Tech. 11* (2006), pp. 1-12

[10] Makinde, O. D., On MHD boundary-layer flow and mass transfer past a vertical plate in a porous medium with constant heat flux, *Int. J. Numer. Methods Heat Fluid Flow, 19* (2009), 3-4, pp. 546-554

[11] Pal, D., Magnetohydrodynamic non-Darcy mixed convection heat transfer from a vertical heated plate embedded in a porous medium with variable porosity, *Commun Nonlinear Sci Numer Simulat., 15* (2010), pp. 3974-3987

[12] Elbashbeshy, E. M. A., Bazid, M. A. A., The Mixed Convection along a Vertical Plate with Variable Surface Heat Flux Embedded in Porous Medium, *Appl. Math. Comp., 125* (2002), pp. 317-324

[13] Kumar, H., Radiative Heat Transfer with Hydromagnetic Flow and Viscous Dissipation over a Stretching Surface in the Presence of Variable Heat Flux, *Thermal Science 13* (2009), 2, pp. 163-169

[14] Eldabe, N. T., Sallam, S. N., MHD Flow and Heat Transfer in a Viscoelastic incompressible fluid confined between a horizontal stretching sheet and a parallel porous wall, *Can. J. Phys., 76* (1998), pp. 949-964

[15] Veena, P. H., *et al.,* Non-Similar Solutions for Heat and Mass Transfer Flow in an Electrically Conducting Visco-Elastic Fluid Over a Stretching Sheet Embedded in a Porous Medium, *Int. J. Modern Mathematics, 2* (2007), 1, pp. 9-26
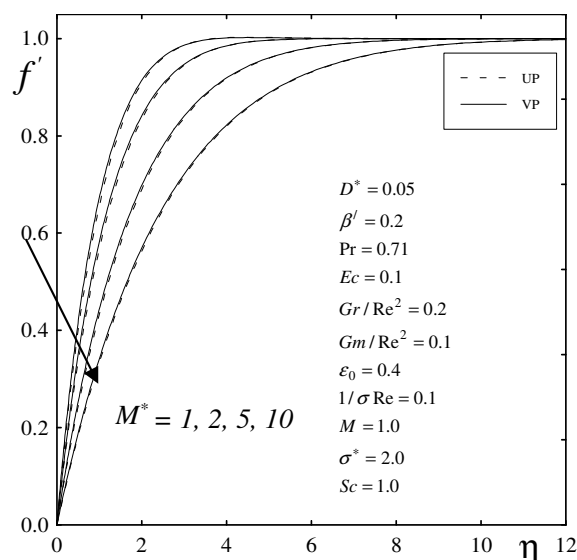
Figure (2). Velocity profiles vs. η for different values of M^*.
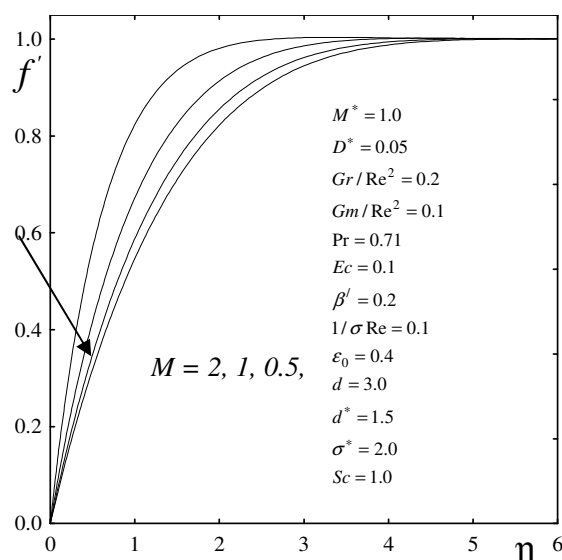
Figure (3). Velocity profiles vs. η for different values of M for VP.

67
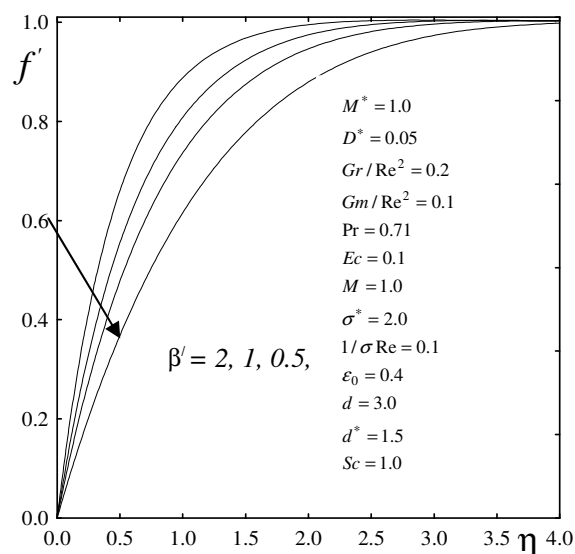
Figure (4). Velocity profiles vs. η for different values of $\beta^{/}$ for VP.
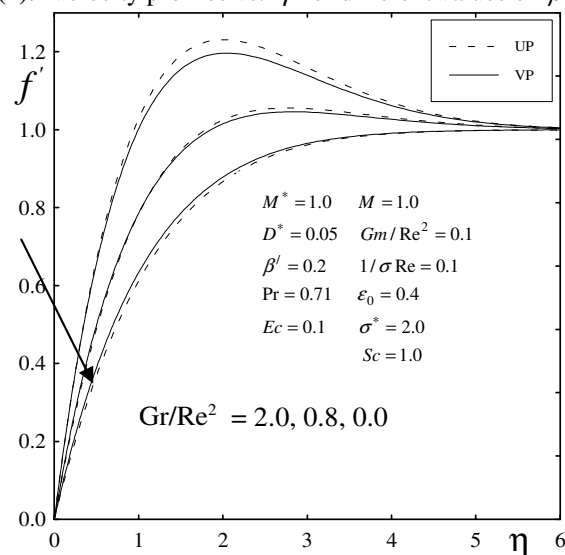
Figure (5). Velocity profiles vs. η for different values of Gr/Re^2.
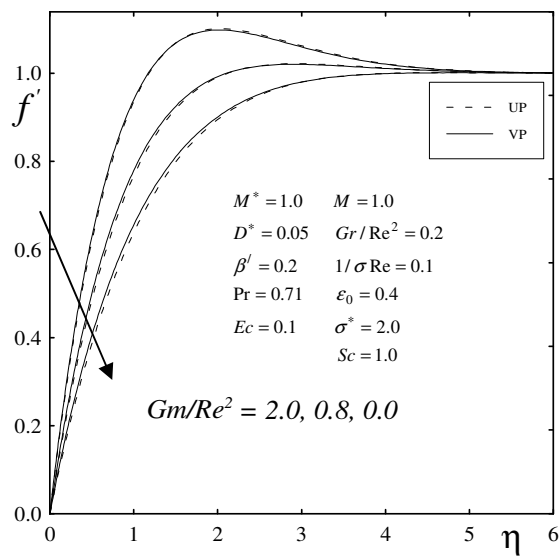
Figure (6). Velocity profiles vs. η for different values of Gm/Re^2.
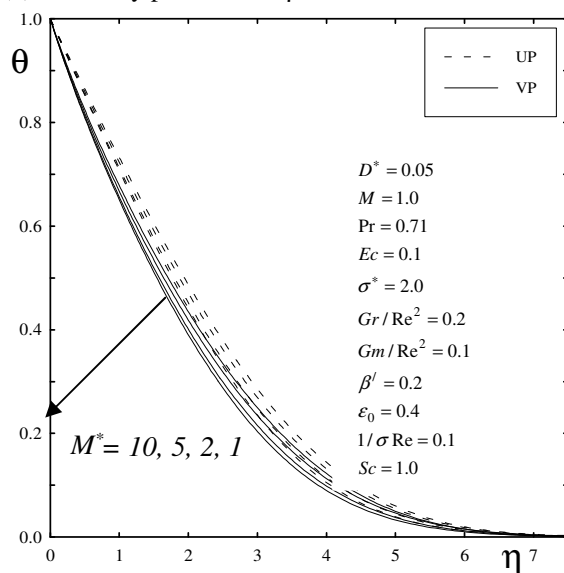
Figure (7). Temperature profiles vs. η for different values of M^*.
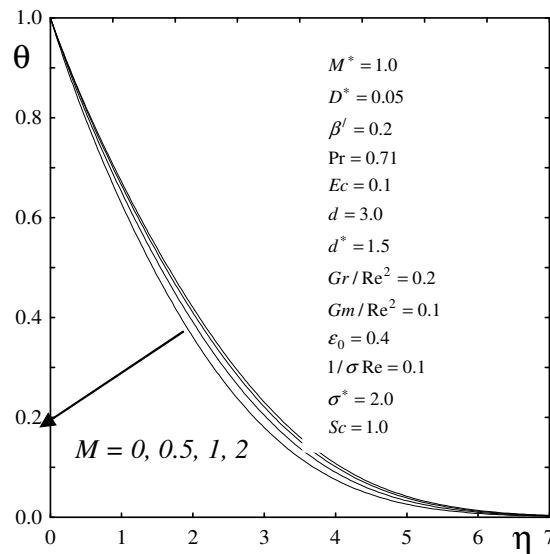
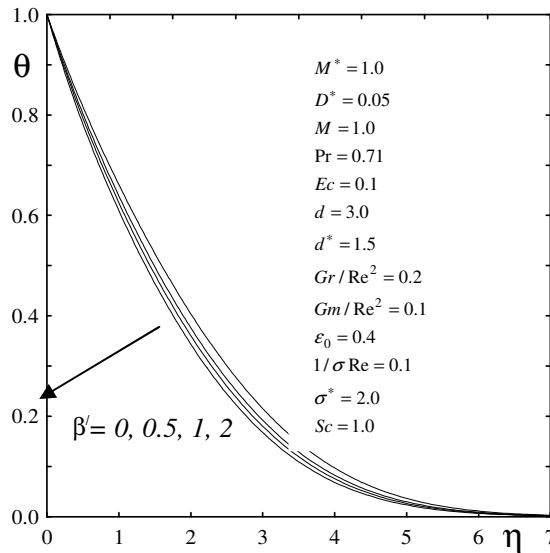**Figure (8).** Temperature profiles vs. η for different values of M for VP.

Figure (9). Temperature profiles vs. η for different values of $\beta^{/}$ for VP.
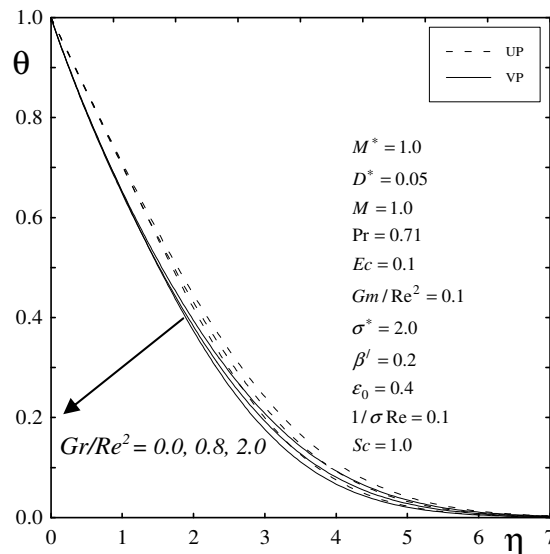
Figure (10). Temperature profiles vs. η for different values of Gr/Re^2.
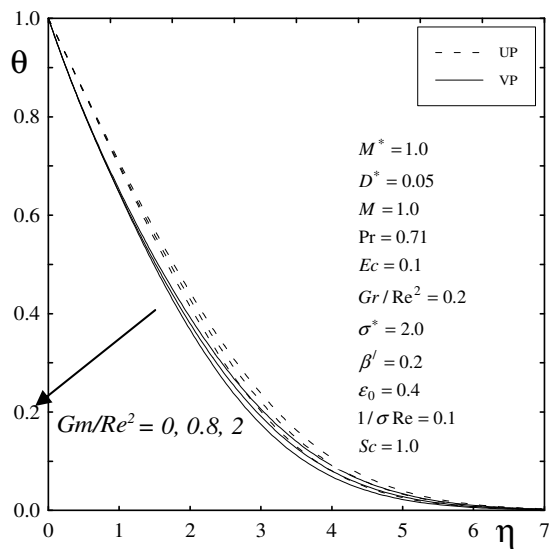
Figure (11). Temperature profiles vs. η for different values of Gm/Re^2.
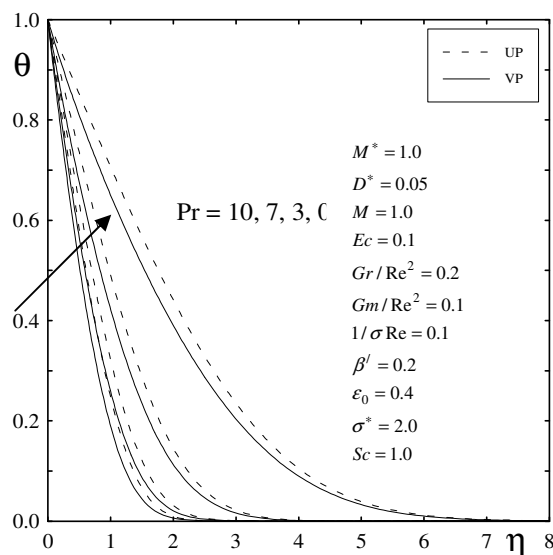
Figure (12). Temperature profiles vs. η for different values of Pr.
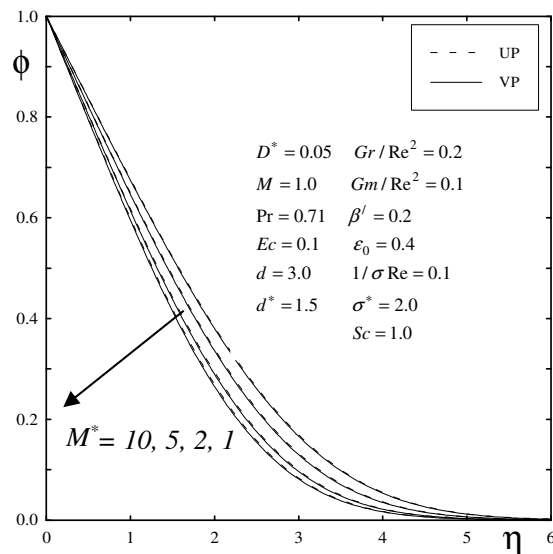
Figure (13). Concentration profiles vs. η for different values of M^*.
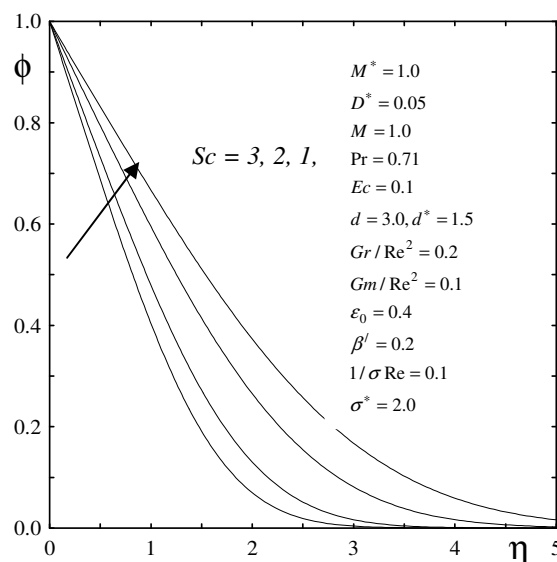
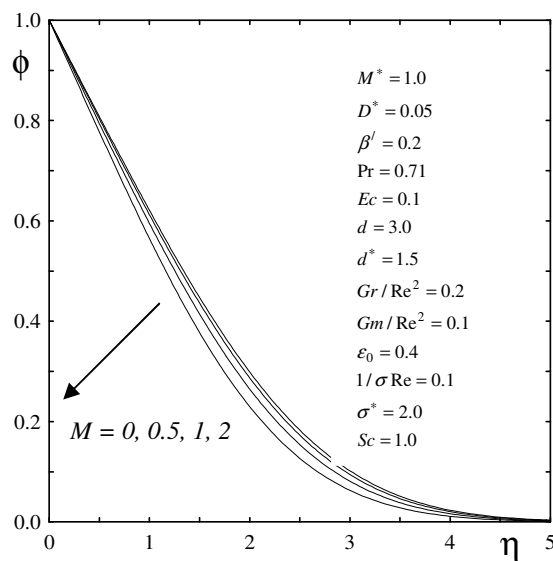**Figure (14).** Concentration profiles vs. η for different values of Sc for VP.

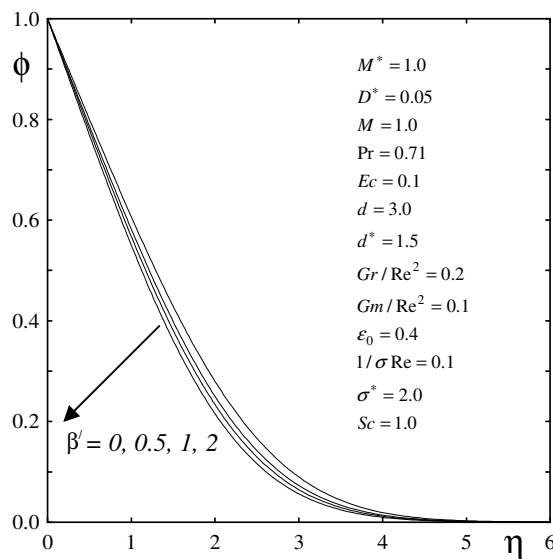**Figure (15).** Concentration profiles vs. η for different values of M for VP.

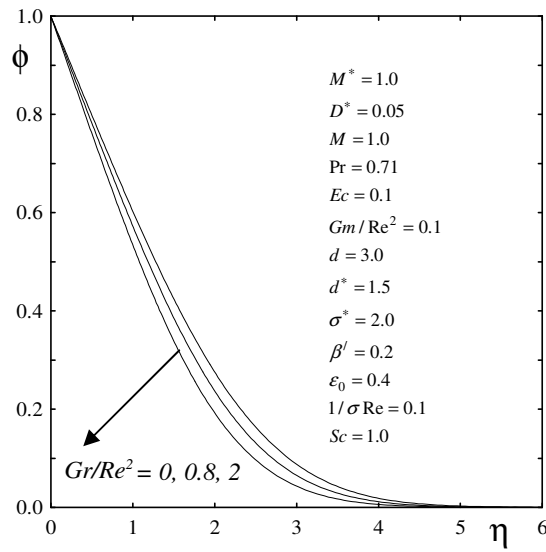**Figure (16).** Concentration profiles vs. η for different values of $\beta^{/}$ for VP.

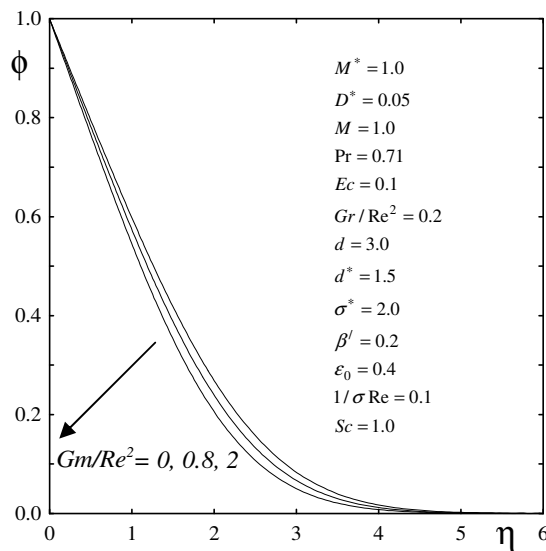**Figure (17).** Concentration profiles vs. η for different values of Gr/Re^2 for VP.

Figure (18). Concentration profiles vs. η for different values of Gm/Re^2 for VP.